

How Observations and Structure Affect the Geostatistical Solution to the Steady-State Inverse Problem

by Peter K. Kitanidis^a

Abstract

The solution to the steady-state inverse problem can be expanded into a series of spline functions with weights adjusted to reproduce the observations within the observation error. The splines depend on the model spatial structure, the ground water flow model, and the location of the observations. This representation of the solution, which is a rigorous and exact expansion, provides insight into the form of the best estimate and explicitly shows how observations and the conceptual model may affect the solution.

Introduction

Consider flow in an aquifer, described by the partial differential equation

$$\frac{\partial}{\partial x_i} \left(T \frac{\partial \phi}{\partial x_i} \right) = -N \quad (1)$$

where T is transmissivity, ϕ is hydraulic head, and N is recharge. T , ϕ , and N may vary in space. Ground water flow models (e.g., McDonald and Harbaugh 1988) are available for the solution of the forward problem: Find ϕ from T , N , and boundary conditions for ϕ . In hydrogeologic applications, an essential part of process simulation is inverse modeling to determine these parameters given available data (Cooley 1977; Poeter and Hill 1997). Inverse methods in hydrogeology are reviewed in Yeh (1986), Ginn and Cushman (1990), Sun (1994), McLaughlin and Townley (1996), and others.

In this work, we will consider the geostatistical approach (Kitanidis and Vomvoris 1983; Dagan 1985; Hoeksema and Kitanidis 1984, 1985, 1989; Rubin and Dagan 1987a, 1987b; Wagner and Gorelick 1989; Kitanidis 1995; Yeh et al. 1996, and others) for the following inverse problem:

Estimate the transmissivity function T given N , boundary conditions for ϕ , and observations of local values of ϕ and perhaps T .

The solution is presented in a form that is favorable for numerical computations and reveals how the observations and the geo-

statistical structure affect the solution. Each observation introduces a basis function or "spline," and the estimate of the unknown is obtained through superposition of such splines. Each of these splines depends on the sensitivity of an observed quantity with respect to the unknown function and the generalized covariance (or variogram) in the geostatistical model. An example is presented to illustrate the application of these concepts.

Overview of Approach

Inverse problems cannot be solved by using observations alone, because observations typically do not provide information sufficient for a unique and stable solution. It is essential to attach information about the degree of variability and spatial continuity (known as "structure") of the unknown function. It is the structure that allows us to obtain a stable solution to an inverse problem. The geostatistical approach is a practical approach to combine observations and structure for the solution of an inverse problem. The unknown function is treated as random, because it is only partially known, and structure is described through the mean and covariance.

The structure of the unknown logtransmissivity (i.e., logarithm of transmissivity) function $s(x) = \ln(T(x))$ is represented through functions with a few adjustable parameters. First, the mean function (also known as drift) that is expanded as

$$\mu(x) = \sum_{i=1}^p X_i(x) \beta_i \quad (2)$$

where $X_i(x)$, for $i = 1, \dots, p$, are known functions and β_i are unknown parameters. A common case is that of a constant but unknown mean: $p = 1$, $X_1(x) = 1$, and thus $\mu(x) = \beta_1$. Second, the covariance function, usually a function of the separation vector, $q(x - x'; \theta)$ where θ are a few parameters (such as variance and

^aDepartment of Civil and Environmental Engineering, Terman Engineering Center, Stanford University, Stanford, CA 94305-4020. E-mail: pkk@ce.stanford.edu

Received June 1997, accepted January 1998.

correlation length) that may need to be adjusted though data analysis. In the inverse modeling presented at the end of this paper, the parameters θ will be estimated using the cross-validation method in Kitanidis (1995).

For notational convenience, the n head and logtransmissivity observations are arranged in a vector, y . Similarly, the unknown function has been discretized into an m by one vector, s . Typically, m is much larger than n . The structure of s is described through a mean vector and a covariance matrix. The mean, following Equation 2, is parameterized into

$$\mu = X\beta \quad (3)$$

where β is the p by one vector of unknown parameters and X is an m by p known matrix, of rank p . The covariance matrix Q is m by m with ij -th element given through the covariance function, $Q_{ij} = q(x_i - x_j; \theta)$. The X and Q matrices depend on the assumed degree of variability and spatial correlation of the unknown function $s(x)$. For more information, see Kitanidis (1995, 1997).

The relation between observations and unknowns is given by the observation equation, with the general form

$$y = h(s) + v \quad (4)$$

The first term, $h(s)$, is the relation between the observations (e.g., head at a certain point) and the unknown function (logtransmissivity). The second term, v , represents observation error and is treated as a random vector with zero mean and covariance matrix R . A priori, s and v are uncorrelated.

In the quasilinear geostatistical approach (Kitanidis 1995), the best estimate \hat{s} is obtained from the minimization of the weighted least squares criterion

$$C = (y - h(\hat{s}))^T R^{-1} (y - h(\hat{s})) + \hat{s}^T G \hat{s} \quad (5)$$

where T indicates matrix transpose and

$$G = Q^{-1} - Q^{-1}X(X^TQ^{-1}X)^{-1}X^TQ^{-1} \quad (6)$$

The first term in Equation 5 represents the objective of reproducing the data within their measurement error and the second term depends on the geostatistical structure. Note that there is no unique minimum if the second term is dropped.

The best estimate \hat{s} must satisfy the normal equation, obtained by setting the derivative of C with respect to s equal to zero,

$$-(y - h(\hat{s}))^T R^{-1}H + \hat{s}^T G = 0 \quad (7)$$

where H is n by m matrix with $H_{ij} = \frac{\partial h_i}{\partial s_j}$. The normal Equation 7 is typically a large system of nonlinear equations.

Consider, first, the case that the observation equation is linear (i.e., the observations are a linear function of s), i.e.,

$$h(s) = Hs \quad (8)$$

the normal equation becomes

$$-(y - H\hat{s})^T R^{-1}H + \hat{s}^T G = 0 \quad (9)$$

The solution is found from the solution of

$$[H^T R^{-1}H + G]\hat{s} = H^T R^{-1}y \quad (10)$$

However, this expression is unsatisfactory because it involves solving systems of order of m , where m can be an arbitrarily large number and the matrix of coefficients is nonsparse.

In our approach, the best estimate is given by

$$\hat{s} = QH^T \xi + Xb \quad (11)$$

where the n by one vector ξ and the p by one vector b are found from the solution of a system of $n + p$ equations with $n + p$ unknowns

$$\begin{bmatrix} \sum HX \\ (HX)^T & 0 \end{bmatrix} \begin{bmatrix} \xi \\ b \end{bmatrix} = \begin{bmatrix} y \\ 0 \end{bmatrix} \quad (12)$$

where

$$\sum = HQH^T + R \quad (13)$$

Solving a single system of $n + p$ equations is much preferable to solving a system of m equations, because typically $m \gg n$. In the examples to be presented later, $n = 50$, $p = 1$ or 3 , and $m = 1200$.

In the more general case that the observation equation is nonlinear, let \tilde{s} be close to the optimal \hat{s} . (In the splines presented later, \tilde{s} will be the true logtransmissivity.) The observation function may be linearized about \tilde{s} , making the normal Equation 7 appear as follows:

$$-(y - h(\tilde{s}) - H(\hat{s} - \tilde{s}))^T R^{-1}H + \hat{s}^T G = 0 \quad (14)$$

or

$$-(\tilde{y} - H\hat{s})^T R^{-1}H + \hat{s}^T G = 0 \quad (15)$$

where

$$\tilde{y} = y - h(\tilde{s}) + H\tilde{s} \quad (16)$$

Equation 15 has the same form as Equation 9. Thus, the solution is

$$\hat{s} = Xb + QH^T \xi \quad (17)$$

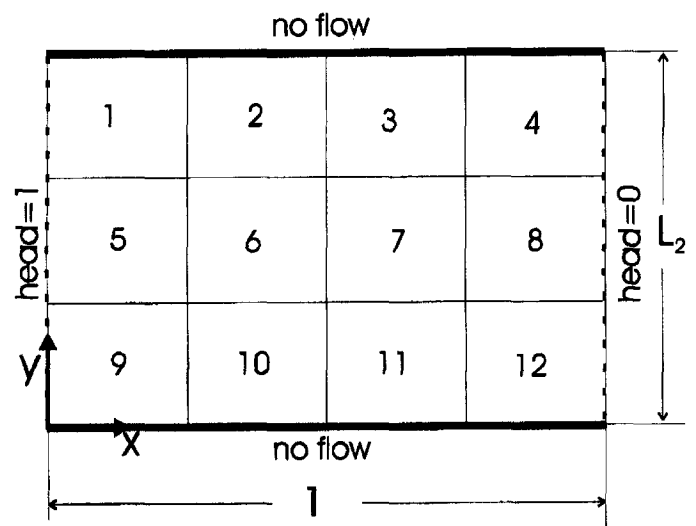


Figure 1. Schematic of flow domain and discretization.

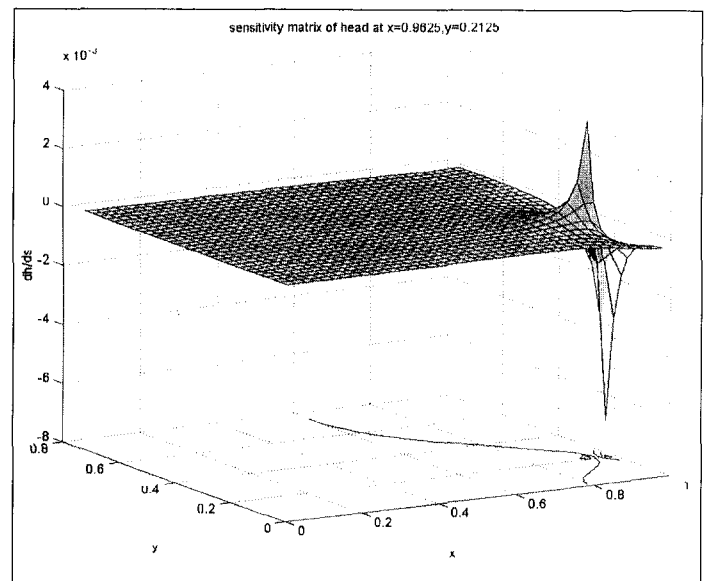
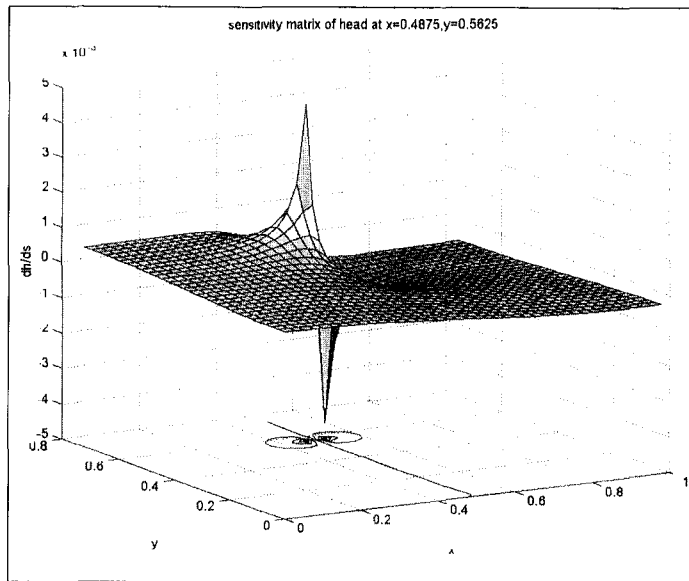


Figure 2. Sensitivity of head at two locations with respect to logtransmissivity. Uniform logtransmissivity, no sources or sinks.

where the ξ and b coefficients are found by solving a single linear system of $n + p$ equations:

$$\begin{bmatrix} \sum \text{HX} \\ (\text{HX})^T & 0 \end{bmatrix} \begin{bmatrix} \xi \\ b \end{bmatrix} = \begin{bmatrix} \bar{y} \\ 0 \end{bmatrix} \quad (18)$$

For weakly nonlinear problems, the Gauss-Newton method of successive linearization is the best iterative method for finding the best estimate. Starting with an initial guess \bar{s} , the observation equation is linearized, Equation 16, and the guess is updated by applying Equations 17 and 18. The procedure is repeated until convergence is achieved.

Consider the best estimate given through Equation 17. This vector is a superposition of $n + p$ vectors multiplied with appropriate coefficients. The $n + p$ vectors are the n columns of matrix QH^T and the p columns of matrix X . The coefficients are the elements of ξ and b , which are found by solving Equation 18. The geostatistical estimate of the unknown function is thus obtained by superposing $n + p$ basis functions or splines with weights adjusted to properly reproduce the data. The splines depend on the observations (type and location) and the assumed geostatistical structure.

The geostatistical structure must be selected on the basis of prior information about the unknown function as well as from the analysis of the data used in the inversion. The objective of this work is to shed light on the question of how structure and observations affect the shape of the splines that are used in the geostatistical solution. This will be achieved by showing plots of splines used in representative examples.

Applications

Consider the rectangular flow domain shown in Figure 1. The left and right boundaries have constant head and the other two are no-flux boundaries. All such cases can be simplified further through nondimensionalization. Distances are normalized by dividing by the length of the domain in the x direction. After this nondimensionalization, the domain is 1 by L_2 , and in the applications presented in this work $L_2 = 0.75$. The head is made dimensionless so that the head is 1 at the left boundary and 0 at the right boundary. The domain is subdivided into m uniform cells with dimensions Δx by

Δy . The logtransmissivity in cell i is s_i , numbered in a row-wise fashion, as illustrated in Figure 1. In the applications, $\Delta x = \Delta y = \frac{1}{40}$ and the grid has 1200 cells.

The forward problem is solved numerically using a cell-centered finite-difference scheme identical to the scheme used in the USGS's popular MODFLOW computer model (McDonald and Harbaugh 1988). The well-known adjoint-state method (Chavent et al. 1975; Neuman 1980) is used to find the sensitivity of a head value (at the center of a cell) with respect to all the transmissivity cells. The sensitivity matrix with respect to the logtransmissivity is then determined through application of the chain rule,

$$\frac{dh}{d(\ln T)} = \frac{dh}{dT} \frac{dT}{d(\ln T)} = \frac{dh}{dT} T \quad (19)$$

Application 1

We will use the expansion of the best estimate \hat{s} into splines, Equation 17, for a given logtransmissivity and recharge. The simplest splines are for the case of uniform logtransmissivity (equal to four in this example) in a domain without recharge or wells. For example, analytical small-perturbation approximations (e.g., Kitanidis and Vomvoris 1983; Dagan 1985) use the splines derived for constant transmissivity without sources or sinks. In this simple case, it is easier to see how the sensitivity functions and the splines associated with observations depend on location and the assumed structure of the unknown.

Figure 2a shows the sensitivity of head at $x = 0.4875$, $y = 0.5625$ to the logtransmissivity function (i.e., the logtransmissivity in every cell). Both the gridded surface and its contour map (appearing on the lowest horizontal plane) are shown. The sensitivity tends to zero away from the head location and its most significant nonzero values are symmetrically located about the head position in the direction of flow. It is worth pointing out that the value of the sensitivity function is grid dependent, because it represents the sensitivity with respect to the logtransmissivity of a cell, and thus changes with the cell size. What matters is the shape of the function; by varying the grid size, we found that the shape of the function is not affected much by discretization. Figure 2b shows the sen-

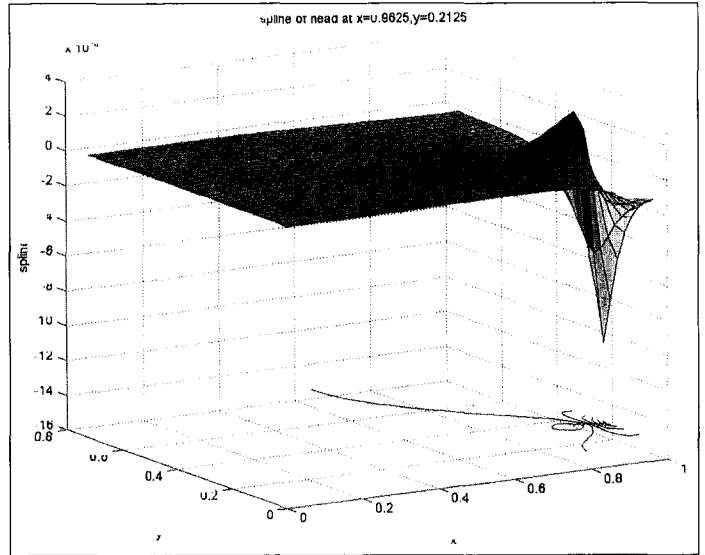
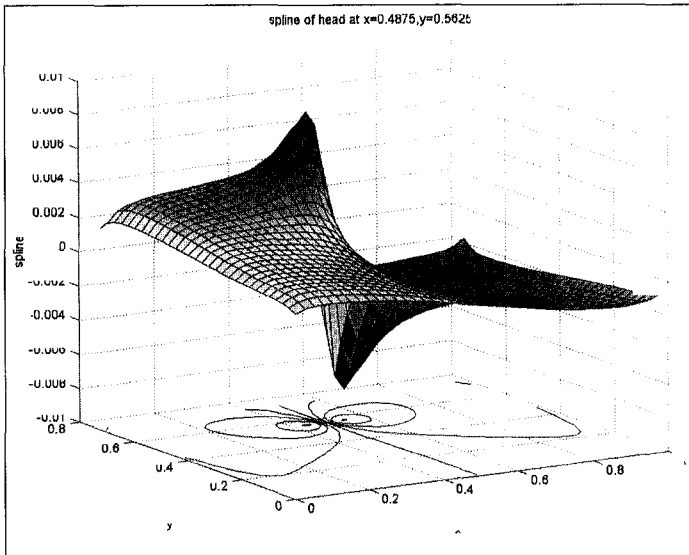


Figure 3. Splines of head at two locations when the exponential covariance function is used with integral scale equal to $\Delta x = 0.025$. Uniform log-transmissivity, no sources or sinks.

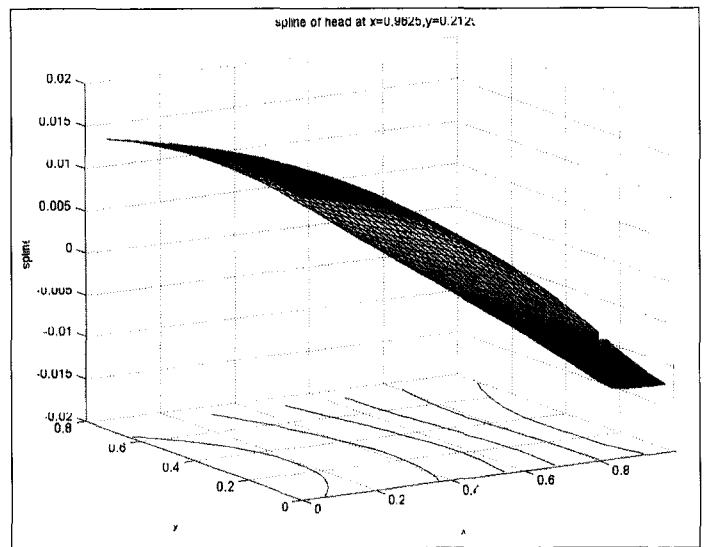
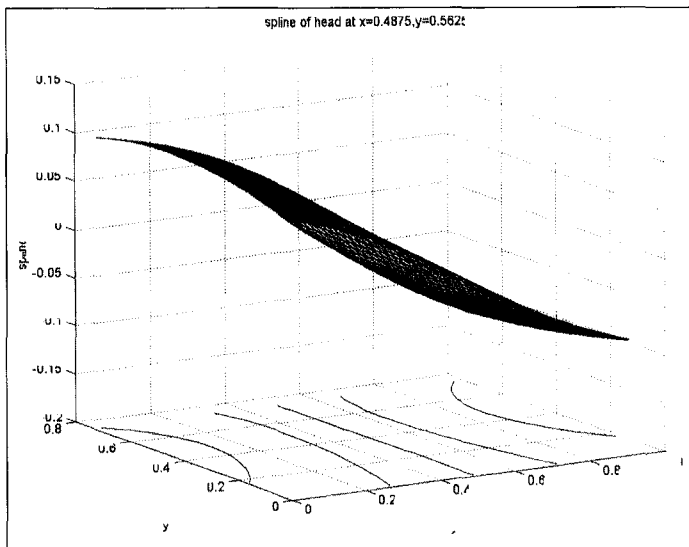


Figure 4. Splines of head at two locations when the linear generalized covariance function is used. Uniform logtransmissivity, no sources or sinks.

sitivity of head at $x = 0.9625$, $y = 0.2125$, near a fixed-head boundary. Due to the boundary proximity, the head is not sensitive to values of the logtransmissivity away from the head location.

The sensitivity functions are identical to the splines used in the inverse problem when the pure nugget effect covariance is used, i.e., constant mean, constant variance, and no correlation between cell values. One expects that the best estimates obtained from an inverse that uses a pure nugget effect model could be spiky and the results might appear “noisy.” A potential advantage of this model is that it does not force any smoothing and thus may allow the identification of small-scale features or abrupt changes in the log-transmissivity. The difficulty is that it is hard to distinguish between actual features and noise.

Figures 3a and 3b show the head splines when the exponential covariance is used,

$$Q_{ij} = \exp\left(-\frac{|x_i - x_j|}{l}\right) \quad (20)$$

where $|x_i - x_j|$ is the distance between cell centers i and j , with spatial coordinates x_i and x_j and l is the integral scale. The spline

shapes, shown in Figures 3a and 3b, differ considerably from the pure nugget effect splines, shown in Figures 2a and 2b, despite the fact that a small $l = \Delta x$ value was used. The larger the value of l , the smoother the spline, which tends to produce a smoother best estimate.

Figures 4a and 4b show the head splines when the linear (generalized) covariance is used,

$$Q_{ij} = -|x_i - x_j| \quad (21)$$

The splines are smooth and appear quite different from the sensitivity functions. Note that in the pure nugget, exponential, and linear models, the X matrix is m by 1 ,

$$X = \begin{bmatrix} 1 \\ 1 \\ \vdots \\ 1 \end{bmatrix} \quad (22)$$

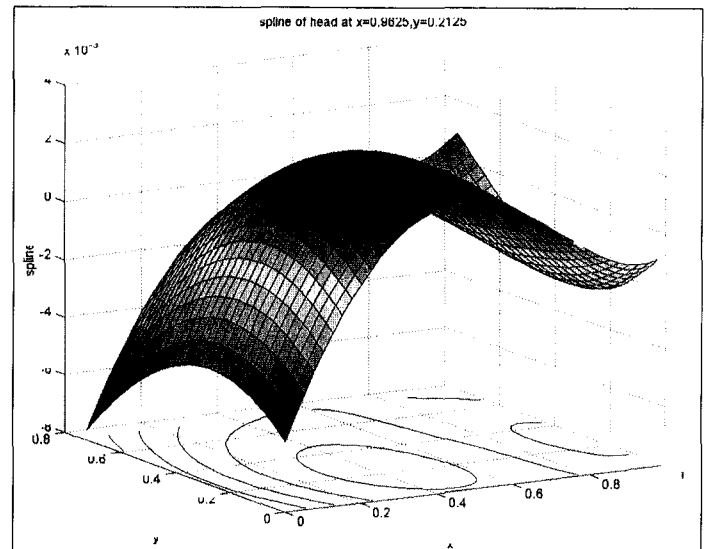
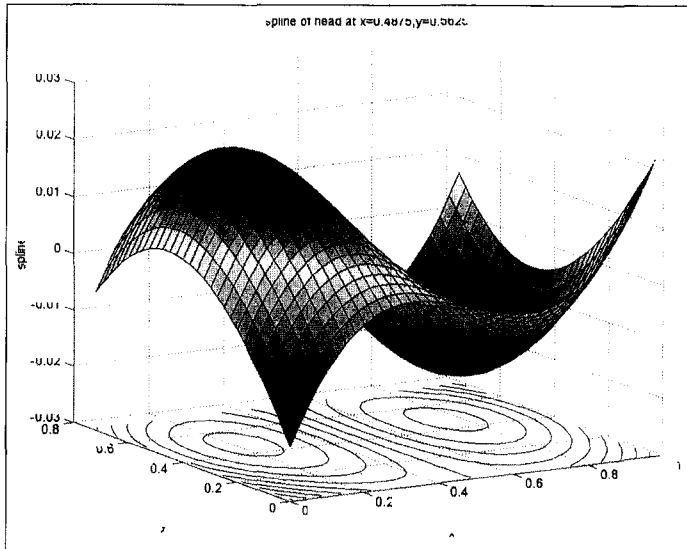


Figure 5. Splines of head at two locations when the thin-plate generalized covariance function is used. Uniform logtransmissivity, no sources or sinks.

A model applicable when there is a linear drift is the thin-plate generalized covariance,

$$Q_{ij} = |x_i - x_j|^2 \log(|x_i - x_j|) \quad (23)$$

The X matrix in this case is m by 3,

$$X = \begin{bmatrix} 1 & x_1 & y_1 \\ 1 & x_2 & y_2 \\ \vdots & \vdots & \vdots \\ 1 & x_m & y_m \end{bmatrix} \quad (24)$$

where (x_i, y_i) are the spatial coordinates of the center of cell i .

Figures 5a and 5b show the head splines associated with this model, which differs even more from the sensitivity matrix. When using this model, a head observation may affect logtransmissivity estimates at large distances.

In all cases, it is the spline geometric shape and not values that matter in determining the best estimate, because in the solution every spline is multiplied by a weight ξ that may be small or large, positive or negative.

Application 2

The shape of the head splines is affected by the presence of distributed recharge or wells. For illustration, consider the case that $N = 0.2$ uniformly over the domain except at two cells, representing production wells, where it is -100 . The wells are at blocks with center coordinates $(0.1125, 0.5125)$ and $(0.6125, 0.5125)$. The value of $\ln T$ is four, just as in Application 1. Figure 6 depicts the head in this case.

Figure 7a and 7b show the head sensitivity functions at the same two locations as in the previous application. The recharge and, more notably, the wells have affected the sensitivity functions. The head may thus be sensitive to values of the logtransmissivity that are strategically located with respect to pumping wells. The best estimates obtained from an inverse that uses a pure nugget effect model could be spiky.

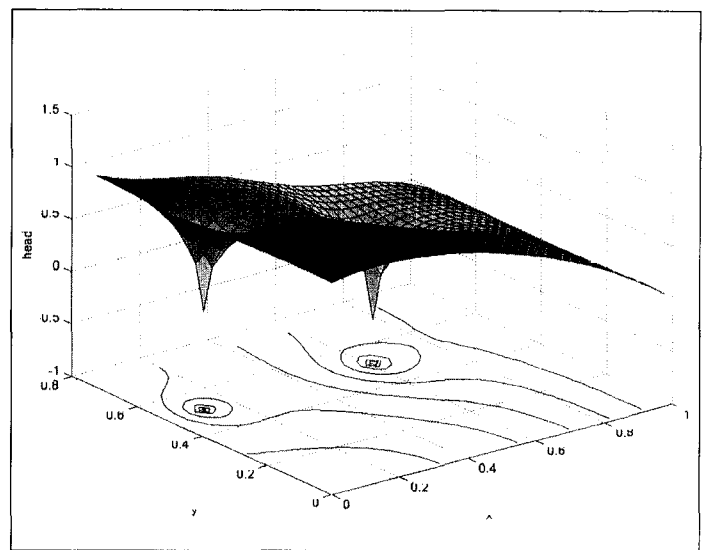


Figure 6. Head for uniform transmissivity, uniform recharge, and two production wells.

Figures 8a and 8b depict the head splines when the exponential covariance is used. Although considerably smoother than the sensitivity functions, the effect of the wells is still pronounced.

Figures 9a and 9b show the head splines with the linear model. The splines are smooth, and the effect of the wells is not immediately obvious.

Figures 10a and 10b show the head splines associated with the thin-plate model. They are smooth and, again, one can see that a head measurement may affect the logtransmissivity estimate at large distances.

Application 3

This is the same as Application 2 with the addition of variable logtransmissivity, shown in Figure 11. Figure 12a and 12b show the head sensitivity functions at the same two locations as in the previous applications. The sensitivity functions have many features now, reflecting the presence of the wells and the permeable zone. The complexity of the sensitivity functions is interesting and reveals how informative an observation may be about hetero-

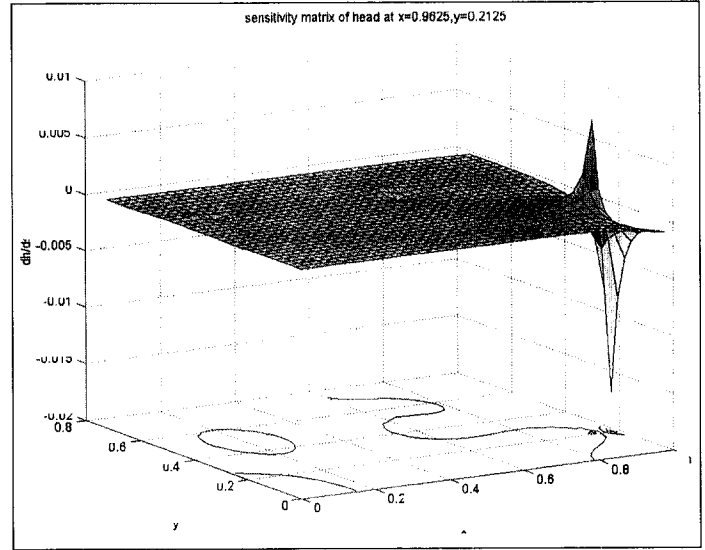
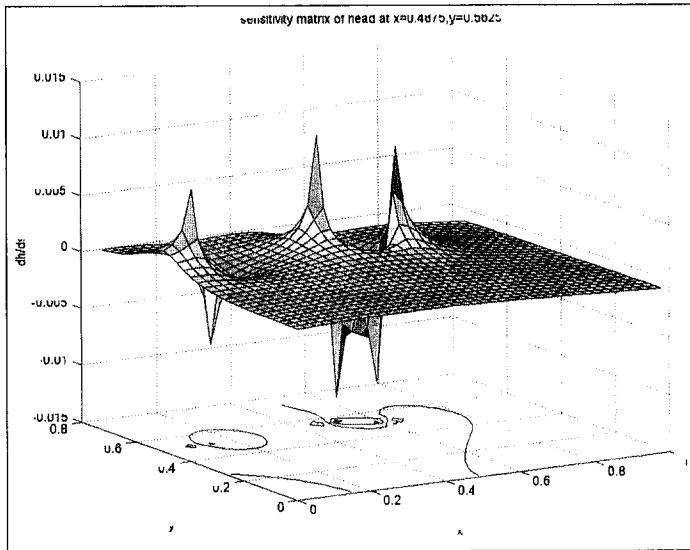


Figure 7. Sensitivity of head at two locations with respect to logtransmissivity. Uniform logtransmissivity.

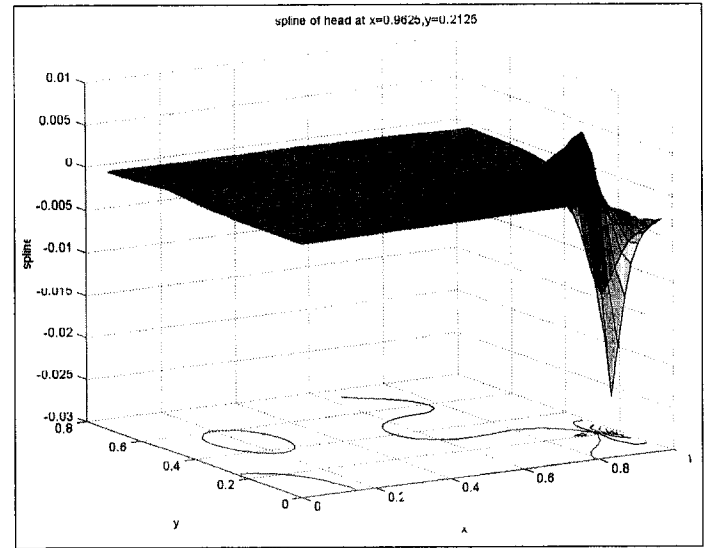
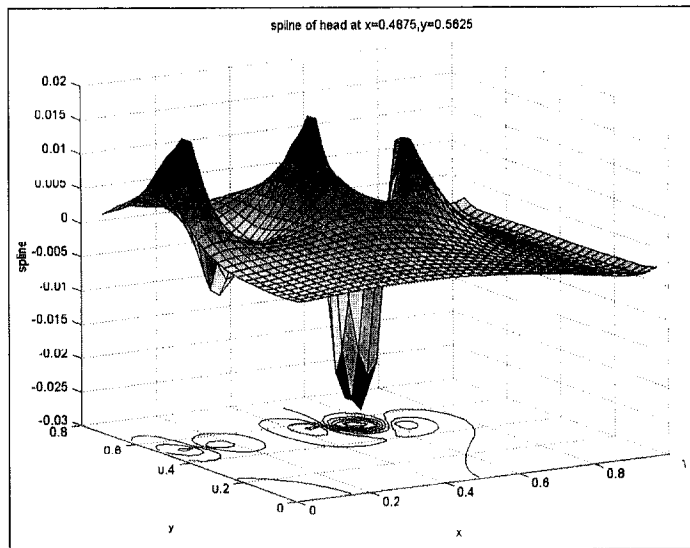


Figure 8. Splines of head at two locations when the exponential covariance function is used with integral scale equal to $\Delta x = 0.025$. Uniform logtransmissivity.

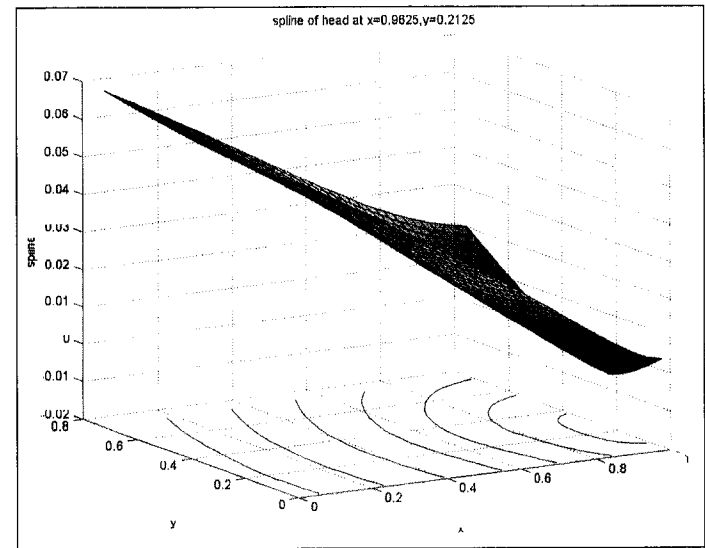
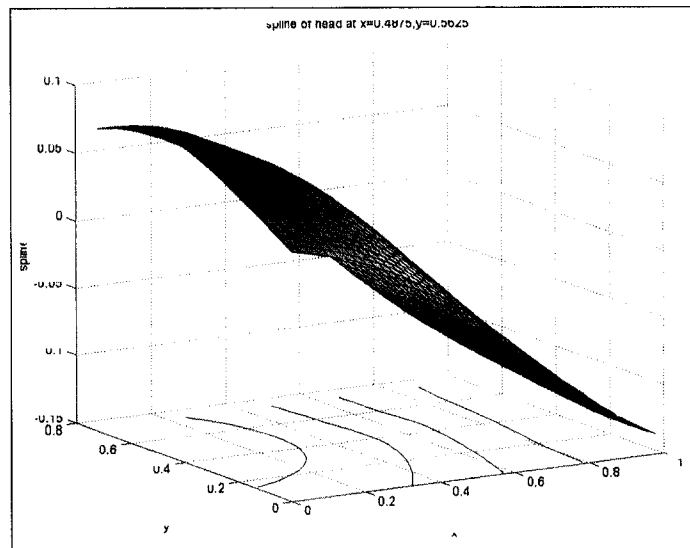


Figure 9. Splines of head at two locations when the linear generalized covariance function is used. Uniform logtransmissivity.

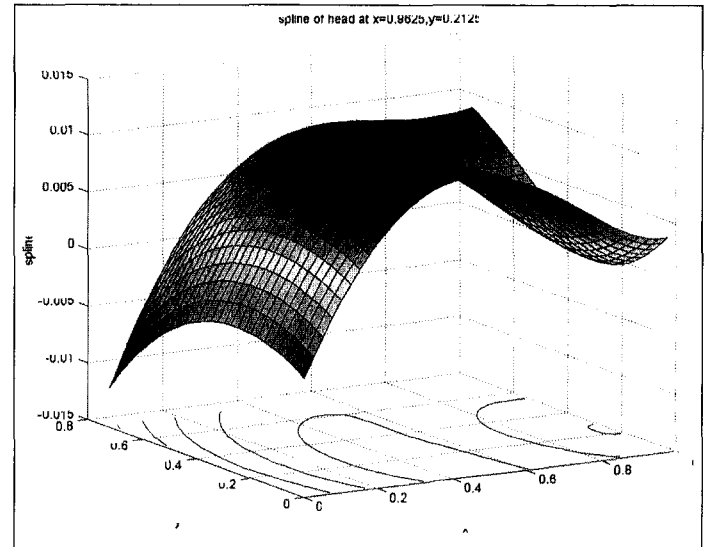
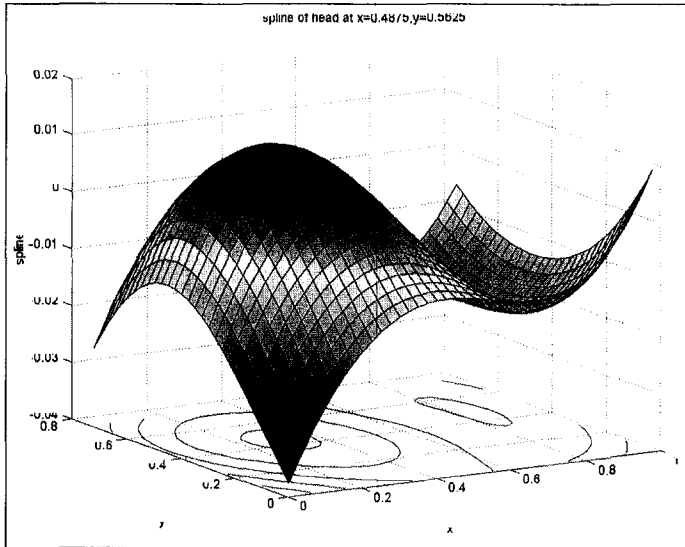


Figure 10. Splines of head at two locations when the thin-plate generalized covariance function is used. Uniform logtransmissivity.

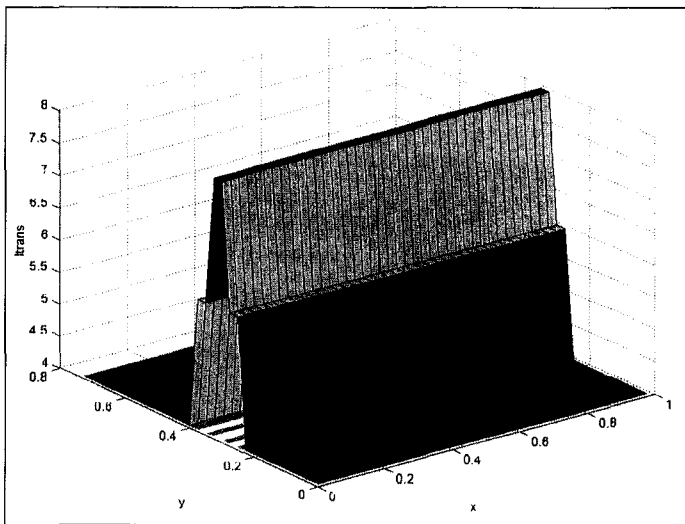


Figure 11. Variable logtransmissivity, used in Application 3.

genities. For example, it is interesting to note that the observation, whose sensitivity is plotted in Figure 12a, is not helpful per se in the detection of the permeable zone. However, the best estimate is computed from the superposition of many splines with appropriately selected coefficients; thus, the right combination of head observations may lead to the detection of the permeable zone.

Figures 13 and 13b depict the head splines using the exponential covariance; Figures 14a and 14b show the head splines using the linear (generalized) covariance; and Figures 15a and 15b show the head splines using the thin-plate model. The splines are dramatically affected by the assumed structure (covariance function). As will be discussed later, the smoothness of the splines used in the linear and thin-plate models may be advantageous.

How do such differences in splines affect the computed best estimate? The answer depends on the specifics of the case. The only general conclusion is that the more observations, the more similar the final estimates. In fact, when every head value is measured, all methods give the same result, regardless of using different splines.

We will show the best estimates for the case when the head is measured at 50 locations, shown in Figure 16. The estimates are obtained using a Gauss-Newton method with θ (parameter multi-

plying each of the covariance functions used in the examples) computed using the method in Kitanidis (1995). The estimates are shown in Figures 17 through 19, for structures given by the exponential, linear, and thin-plate models. The exponential model estimate is somewhat bumpy (because of the small integral scale used) but captures the main feature of the flow domain, that is, the permeable zone near the center. The linear model estimate is relatively flat and the thin-plate estimate is relatively smooth and somewhat wavy. The thin-plate spline is expected to work well for logtransmissivity functions that have continuous first derivatives, a condition not met in this example.

In this case, the linear model estimate is more accurate than the other two estimates. It is interesting to note that the simplicity of the linear model splines has not prevented the identification of the most important real site features; at the same time, the estimate is free of features that appear in the exponential model estimate but are not real. However, all three solutions share common characteristics: They are able to identify the thick permeable zone, but not the thinner interior one. The reason is that when head observations are used, one cannot estimate logtransmissivity features that are smaller than the average distance between head observations. Typically, small-scale characteristics of the logtransmissivity functions are smoothed out. Introducing a weak spatial correlation is generally not a good approach to identify small-scale characteristics. For example, in the exponential model with $l = \Delta x$, the result is a bumpy solution, most of the bumps being spurious features and not real site characteristics.

Concluding Remarks

The best estimate of the logtransmissivity that is obtained from the solution of an inverse problem is a smoothed version of the actual logtransmissivity. The estimate can be expanded into a series of spline functions with appropriate weights, Equation 17. This expansion is an exact representation, unlike ad hoc approximations used in other approaches. The shape of the splines turns out to depend on the geostatistical structure, the flow model, and the location and type of observations. For example, the spline associated with a head observation is different from the spline associated with a logtransmissivity observation. These splines show how an observation affects the estimate and thus are useful

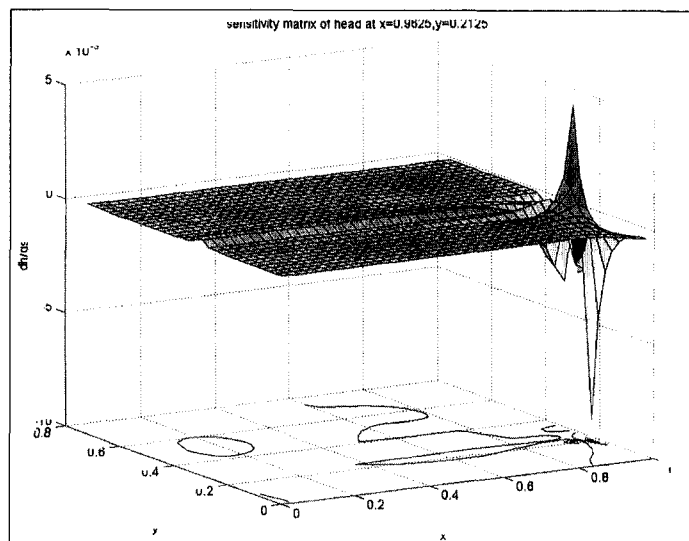
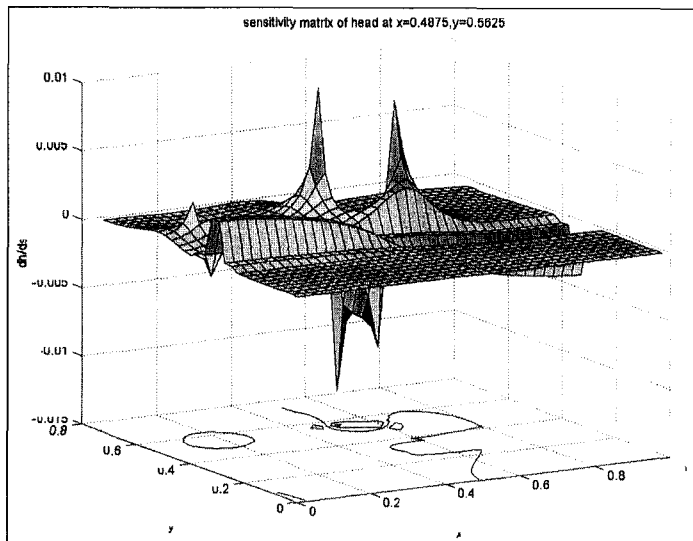


Figure 12. Sensitivity of head at two locations with respect to logtransmissivity.

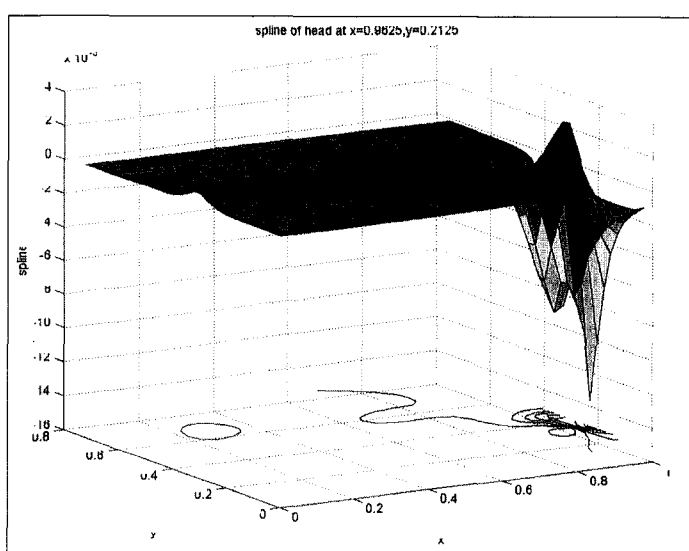
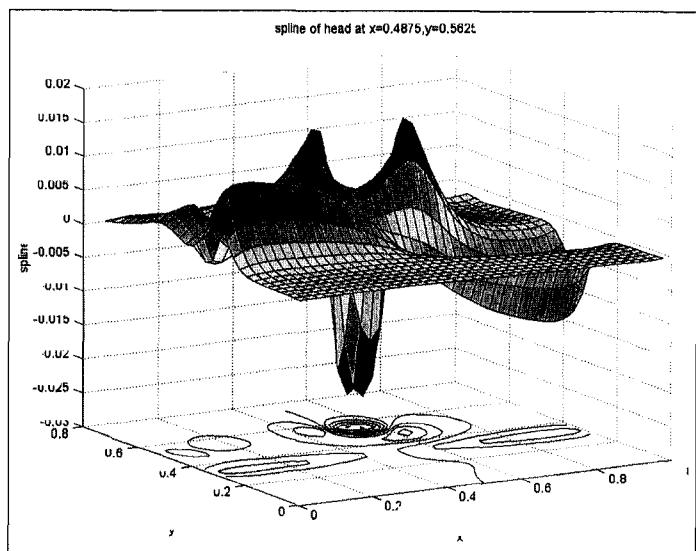


Figure 13. Splines of head at two locations when the exponential covariance function is used with integral scale equal to $\Delta x = 0.025$.

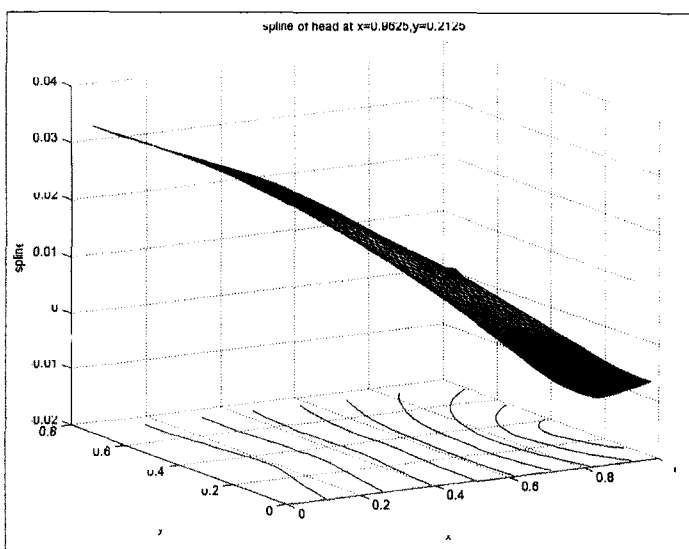
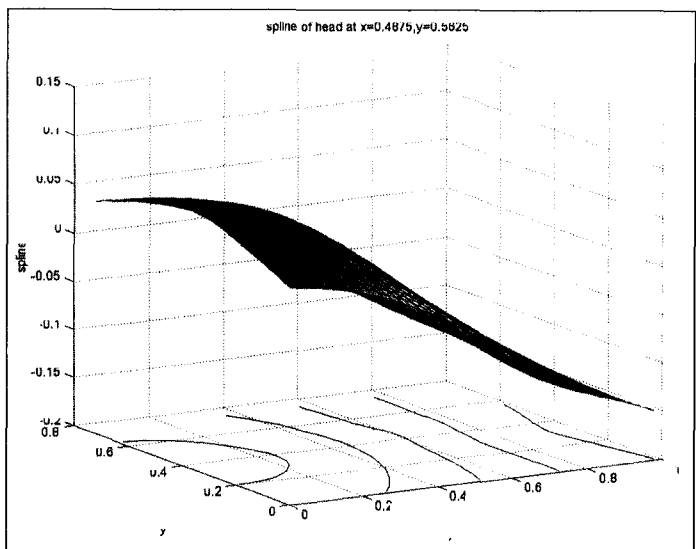


Figure 14. Splines of head at two locations when the linear generalized covariance function is used.

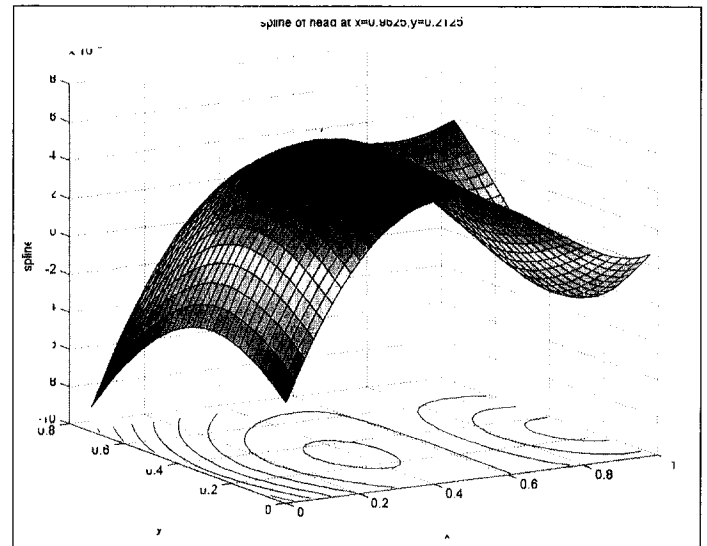
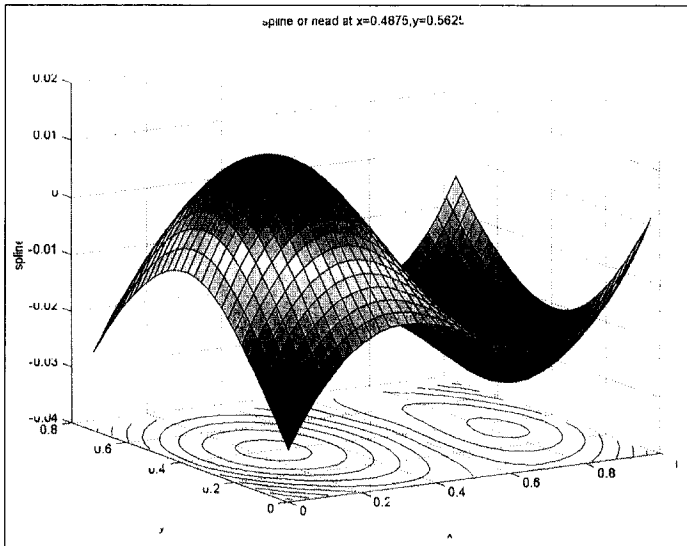


Figure 15. Splines of head at two locations when the thin-plate generalized covariance function is used.

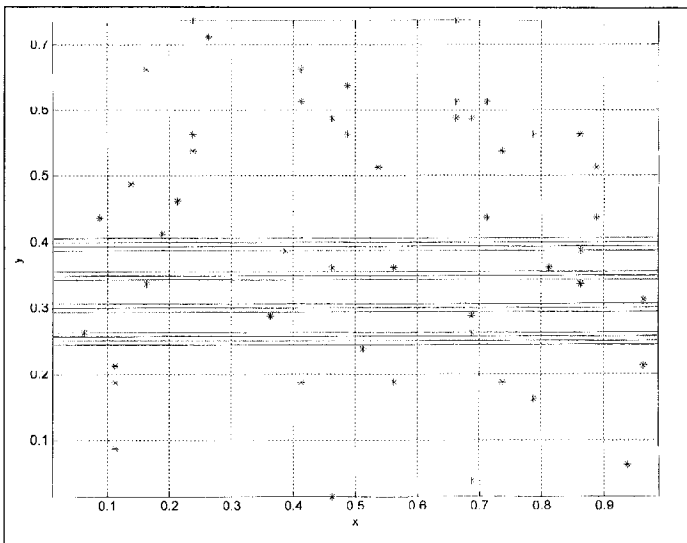


Figure 16. Contour map of logtransmissivity and locations of head observations (shown by *).

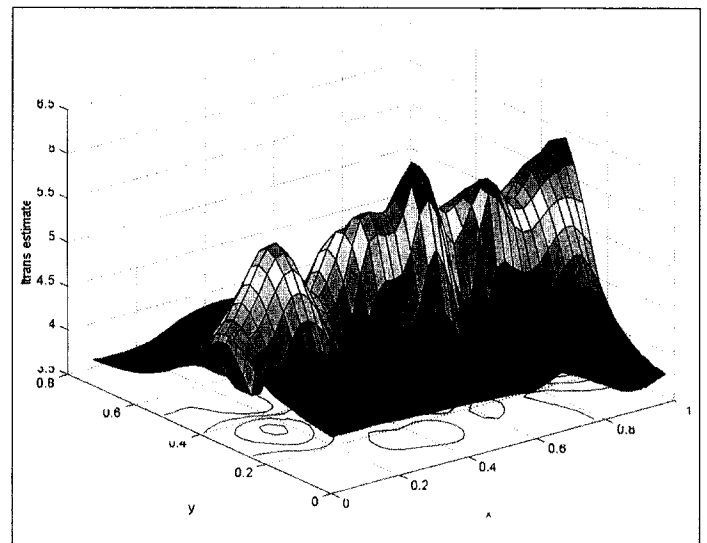


Figure 18. Best estimate of logtransmissivity using the linear model.

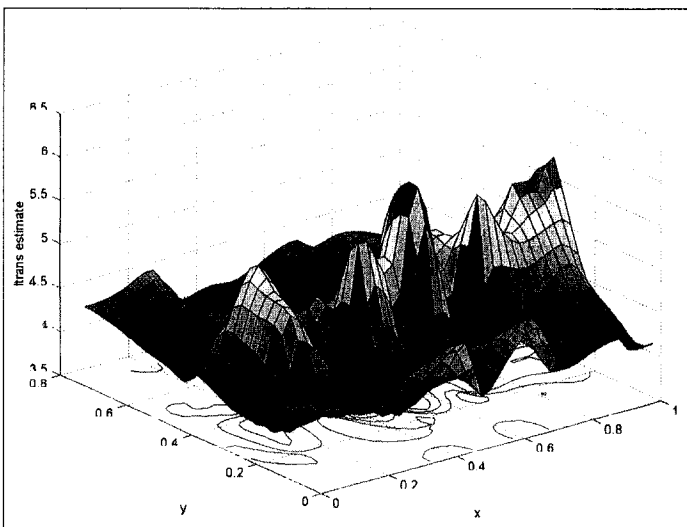


Figure 17. Best estimate of logtransmissivity using the exponential model with $l = \Delta x$.

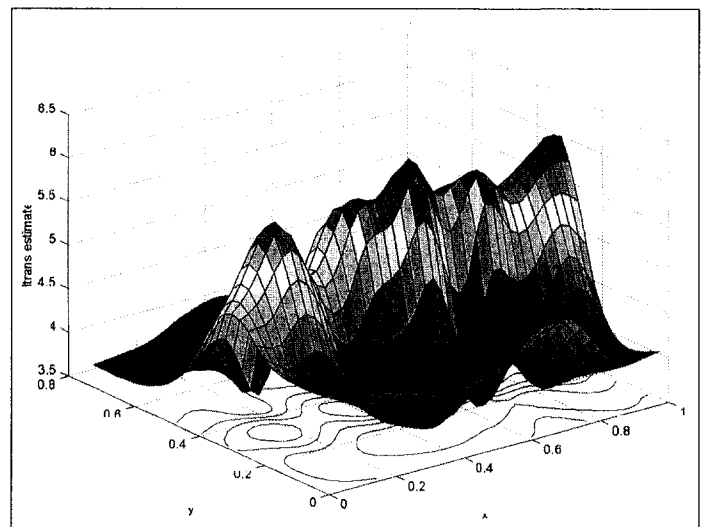


Figure 19. Best estimate of logtransmissivity using the thin-plate model.

in understanding what measurements are responsible for the identification of a given feature or in considering what measurements to collect next.

An interesting feature is that the geostatistical structure has a major effect on the shape of the individual splines. The stronger the spatial continuity, the smoother the splines. Additionally, there is a fundamental trade-off between riding the estimate of spurious variability and sacrificing some of the resolution of the actual log-transmissivity. The challenge is to find the degree of spatial continuity and smoothness that strikes an acceptable balance between suppressing errors and identifying actual features of spatial variability.

Acknowledgments

Funding for this work was provided by the office of Research and Development, U.S. Environmental Protection Agency, under agreement R-815738-01 through the Western Region Hazardous Substance Research Center. The content of this study does not necessarily represent the views of the agency. The forward problem and adjoint state subroutines were skillfully programmed by Menelaos Karavelas.

References

- Chavent, G., M. Dupuy, and P. Lemoigner. 1975. History matching by use of optimal theory. *Soc. Pet. Eng. J.* 15, no. 1: 74-86.
- Cooley, R.L. 1977. A method for estimating parameters and assessing reliability for models of steady state groundwater flow, 1. Theory and numerical properties. *Water Resour. Res.* 13, no. 2: 318-324.
- Dagan, G. 1985. Stochastic modeling of groundwater flow by unconditional and conditional probabilities: The inverse problem. *Water Resour. Res.* 21, no. 1: 65-73.
- Ginn, T.R., and J.H. Cushman. 1990. Inverse methods for subsurface flow: A critical review of stochastic techniques. *Stoch. Hydrol. Hydraul.* 4, no. 1: 1-26.
- Hoeksema, R.J., and P.K. Kitanidis. 1984. An application of the geostatistical approach to the inverse problem in two-dimensional groundwater modeling. *Water Resour. Res.* 20, no. 7: 1003-1020.
- Hoeksema, R.J., and P.K. Kitanidis. 1985. Comparison of Gaussian conditional mean and kriging estimation in the geostatistical solution of the inverse problem. *Water Resour. Res.* 21, no. 2: 825-836.
- Hoeksema, R.J., and P.K. Kitanidis. 1989. Prediction of transmissivities, heads, and seepage velocities using mathematical models and geostatistics. *Adv. in Water Resour.* 12, no. 2: 90-102.
- Kitanidis, P.K., and E.G. Vomvoris. 1983. A geostatistical approach to the inverse problem in groundwater modeling (steady state) and one-dimensional simulations. *Water Resour. Res.* 19, no. 3: 677-690.
- Kitanidis, P.K. 1995. Quasilinear geostatistical theory for inverting. *Water Resour. Res.* 31, no. 10: 2411-2419.
- Kitanidis, P. K. 1997. *Introduction to Geostatistics*. Cambridge, United Kingdom: Cambridge University Press.
- McDonald, M.G., and A.W. Harbaugh. 1988. A modular three-dimensional finite-difference ground-water flow model. U.S. Geological Survey Techniques of Water-Resources Investigations, Book 6, Chap. A1.
- McLaughlin, D., and L.R. Townley. 1996. A reassessment of the groundwater inverse problem. *Water Resour. Res.* 32, no. 5: 1131-1161.
- Neuman, S.P. 1980. Adjoint-state finite element equations for parameter estimation. In *Finite Elements in Water Resources: Proceedings of Third International Conference*, ed. S. W. Wang, C.V. Alonso, C.A. Brebbia, W.G. Gray, and G.F. Pinder. New York: Springer-Verlag.
- Poeter, E.P., and M.C. Hill. 1997. Inverse models: A necessary next step in groundwater modeling. *Ground Water* 35, no. 2: 250-260.
- Rubin, Y., and G. Dagan. 1987a. Stochastic identification of transmissivity and effective recharge in steady groundwater flow, 1. Theory. *Water Resour. Res.* 23, no. 7: 1185-1192.
- Rubin, Y., and G. Dagan. 1987b. Stochastic identification of transmissivity and effective recharge in steady groundwater flow, 2. Case study. *Water Resour. Res.* 23, no. 7: 1193-1200.
- Sun, N.-Z. 1994. *Inverse Problems in Groundwater Modeling*. Norwell, Massachusetts: Kluwer.
- Wagner, B.J., and S.M. Gorelick. 1989. Reliable aquifer remediation in the presence of spatially variable hydraulic conductivity: From data to design. *Water Resour. Res.* 25, no. 10: 2211-2225.
- Yeh, W.W.-G. 1986. Review of parameter identification procedures in groundwater hydrology: The inverse problem. *Water Resour. Res.* 22, no. 1: 95-108.
- Yeh, J.T.-C., M. Jin, and S. Hanna. 1996. An iterative stochastic inverse method: Conditional effective transmissivity and hydraulic head fields. *Water Resour. Res.* 32, no. 1: 85-92.